Asymmetrical Wake Generated by a Spinning Cylinder

F. Diaz* and J. Gavaldà†
University of Barcelona, Tarragona, Spain

J. G. Kawall‡ and J. F. Keffer§
University of Toronto, Toronto, Canada

and

F. Giralt¶
University of Barcelona, Tarragona, Spain

An extended set of measurements has been carried out on a developing turbulent wake behind a spinning circular cylinder immersed in a uniform stream. Various moments of the velocity signals have revealed the effect of the rotation upon characteristic parameters of the flowfield. For small values of rotation, where the circumferential velocity is less than the freestream velocity, a quasiconventional turbulent wake behavior obtains. At high values of rotation, the magnitudes of all dynamic turbulent fluctuations decrease substantially due to the suppression of the Kármán vortex street. As well, it was observed that a region of negative production was generated in the developed flow for those cases where the circumferential velocities were comparable to the freestream velocity. This aspect is explored in considerable detail.

Nomenclature

C_D = drag coefficient
D = cylinder diameter
e = displacement size
L = cylinder length
ℓ_0 = characteristic wake width
n = frequency
n_S = Strouhal frequency
$\overline{q^2}$ = twice the turbulent kinetic energy
R_{uv} = correlation coefficient
Re = Reynolds number
S = Strouhal number
u, v = fluctuating velocities
U = streamwise mean velocity
U_m = minimum value of streamwise mean velocity
U_0 = potential velocity
U_p = peripheral velocity of the rotating cylinder
$\overline{uv}$ = Reynolds shear stress
x, y = streamwise and lateral coordinates
y^+, y^- = lateral positions of maximum positive and negative shear stress
y_c = lateral position of the centerline
y_m = lateral position of the maximum velocity defect
ΔU_m = maximum value of the mean velocity defect
π = turbulent kinetic energy total production term

Introduction

In recent years, there has been a growing body of experimental data indicating that most, if not all, asymmetric turbulent flows are anomalously different from their symmetric counterparts. Specifically, it has been observed that the presence of asymmetry in the mean intensity profiles of either velocity or temperature fields can generate regions where the product of the turbulent fluctuation stress and intensity gradient quantities produces a negative turbulent kinetic energy term or its thermal equivalent. If this is of high enough magnitude, the total turbulent kinetic energy production within this region can be negative.[1-6] The implication of this is that it is necessary to change the conventional modeling of the turbulent transport mechanism. Further work[6,7] has shown that the anomalous transport is closely linked to the presence of at least two distinct sizes of coherent structures within these flows.

The present experimental investigation of the wake behind a spinning cylinder has been undertaken in an attempt to obtain more information about the dynamics of turbulent motion in asymmetric flows and to determine how this is affected by the presence of distinct coherent structures such as Kármán vortices that have been modified by the flowfield. We note that this flow has technological significance with respect to the generation of electrical power by means of wind turbines.

Experimental Considerations

The flow examined here was generated in a variable-speed open-circuit wind tunnel, which is located in the Department de Química Tècnica, Universitat de Barcelona, Tarragona. This tunnel has a $0.6 \times 0.6 \times 3.0$ m test section and is equipped with a portable traversing mechanism, comprising a vertical shaft and a sleeve and gear assembly, that allows a probe to be positioned inside the test section to within ± 0.1 mm, or approximately ± 0.005 D, in the y direction (see Fig. 1). A detailed description of the tunnel and the traversing mechanism is given in Ref. 8.

The wake, which is shown schematically in Fig. 1, was produced by means of a circular cylinder of diameter D equal to 19.7 mm and a length L equal to the width of the tunnel (viz., 0.6 m), so that the L/D ratio was in excess of 30. Mean velocity data obtained in (x-y) planes parallel to the vertical centerplane of the tunnel indicated that this L/D value was sufficiently large to insure that the central region of the flow was essentially two dimensional at all stations (i.e., x/D locations) examined herein. The cylinder was mounted hori-

Received July 7, 1983; revision received Dec. 5, 1984.

*Assistant Professor, Departaments de Química Tècnica i Fisica, Facultat de Química.
†Assistant Professor, Departaments de Química Tècnica i Física, Facultat de Química.
‡Associate Professor, Department of Mechanical Engineering.
§Professor, Department of Mechanical Engineering.
¶Professor, Departaments de Química Tècnica i Física, Facultat de Química.

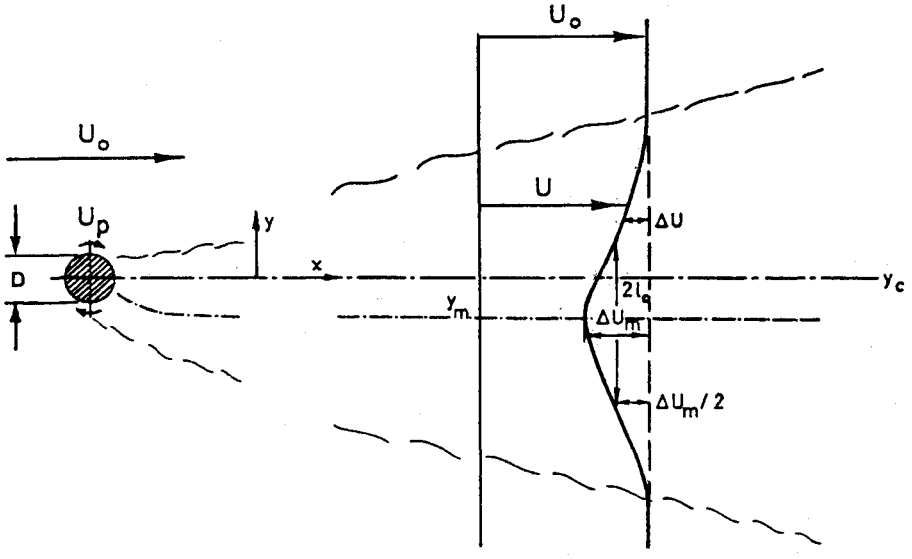

Fig. 1 Definition sketch.

zontally in the center of the tunnel and supported in bearings attached to the tunnel walls, with one end connected to a variable-speed motor, so that it could be rotated at selected speeds U_p, which were measured with the aid of a stroboscope. The tunnel was operated at a speed U_0 of 7 ms^{-1}, which produced a cylinder Reynolds number of about 9000. Measurements were performed in the vertical centerplane of the tunnel at a number of downstream locations corresponding to x/D values between 3 and 150. Instantaneous streamwise and lateral velocities were obtained by means of DISA 55M constant-temperature anemometers in conjunction with two normal hot-wire probes orientated so that their wires were at 90 deg to U_0 and a 45 deg X-wire probe orientated so that its wires were at 45 deg to U_0. The probes were supported by (horizontal) DISA hot-wire mounting tubes that could be attached to the aforementioned traversing mechanism. The analog voltages from the anemometers were low-pass filtered at 2 kHz to insure that the measured signals contained only the relevant turbulence Fourier components. For the purpose of carrying out spectral and correlation analyses, the signals were digitalized at a sampling rate of 7042 points/s and subsequently processed with the aid of FORTRAN IV software on an IBM digital computer at the University of Toronto. Mean velocities were checked via a pitot-static tube combined with a differential-pressure cell transducer.

Preliminary measurements[8] indicated that the curvature of the mean streamlines of the flow that resulted when U_p/U_0 was significantly greater than zero was negligibly small for x/D in excess of about 2.5, signifying that the mean direction of the flow was essentially the same as that of the freestream for all stations examined. Accordingly, it was possible to determine the streamwise and lateral velocity signals (and their statistical properties) pertaining to these stations from the measured anemometer voltage signals.

The Mean Velocity Field

The development of the mean velocity field of the wake pertaining to cylinder peripheral velocities equal to 0, 1.0, and 2.5 times the freestream velocity is illustrated in Fig. 2. With respect to the stationary cylinder situation ($U_p/U_0 = 0$), the velocity profiles are symmetrical around the position of the central plane y_c for all stations and are in agreement with published data. As U_p/U_0 increases, however, these profiles become increasingly asymmetrical, especially in the near-wake region, and the lateral positions y_m where the maximum values of the mean velocity defect occur are laterally displaced in a direction consistent with the sense of the cylinder rotation, signifying that there is a net lateral (i.e., downward)

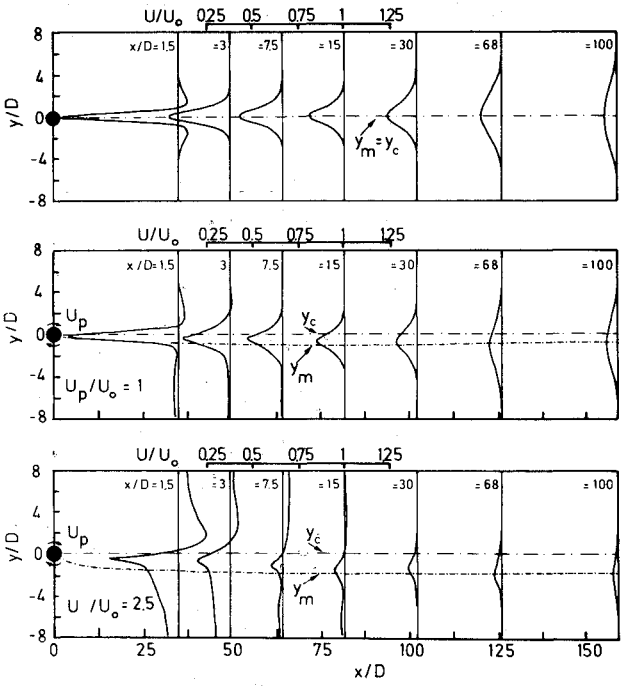

Fig. 2 Mean streamwise velocity distributions.

transfer of momentum within the wake. This momentum transfer is balanced by the lift force acting on the rotating cylinder, which is the so-called Magnus effect. It should be mentioned that the direction of the momentum transfer reverses slightly further downstream as a consequence of the expansion of the initially highly compressed streamlines within the lower region of the flow, which is associated with the bottom of the cylinder where the direction of the peripheral velocity is opposite that of the freestream. For all peripheral velocities, the characteristic wake width increases and the maximum velocity defect decreases with increasing x/D, because of the diffusional processes that take place in any free turbulent shear flow. Moreover, as a result of the cylinder rotation, the acceleration of the fluid beyond U_0 in the near-wake region, which is caused by the presence of the cylinder and occurs at $x/D \leq 3$ when $U_p/U_0 = 0$, is enhanced in the upper region of the flow associated with the top of the cylinder. Here the direction of U_p is the same as that of U_0 and is suppressed or even reversed in the lower region associated with the bottom of the cylinder, where the direction of U_p

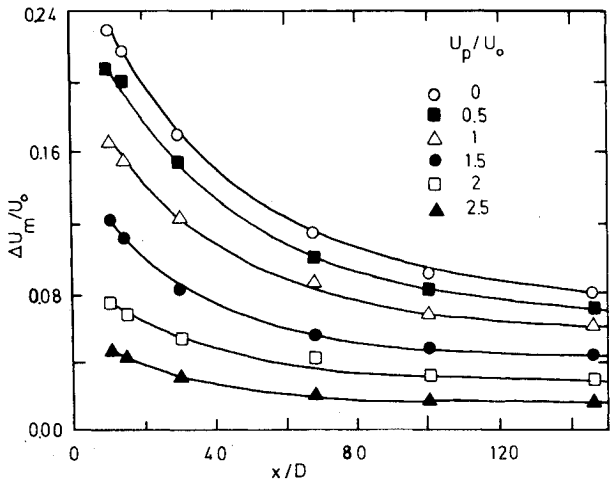

Fig. 3 Longitudinal variation of the maximum value of mean velocity defect.

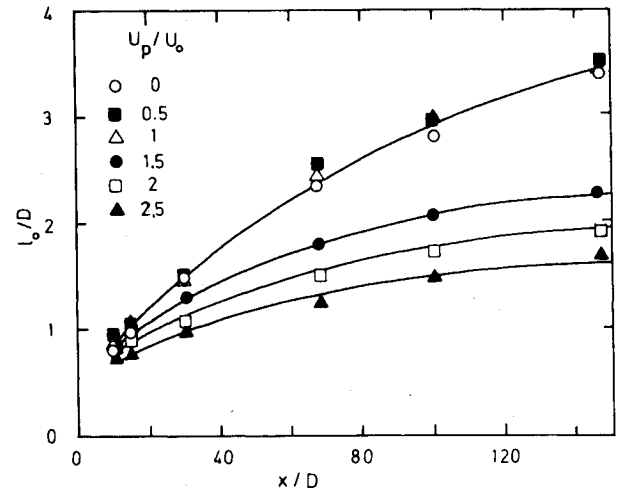

Fig. 4 Longitudinal variation of the characteristic wake width.

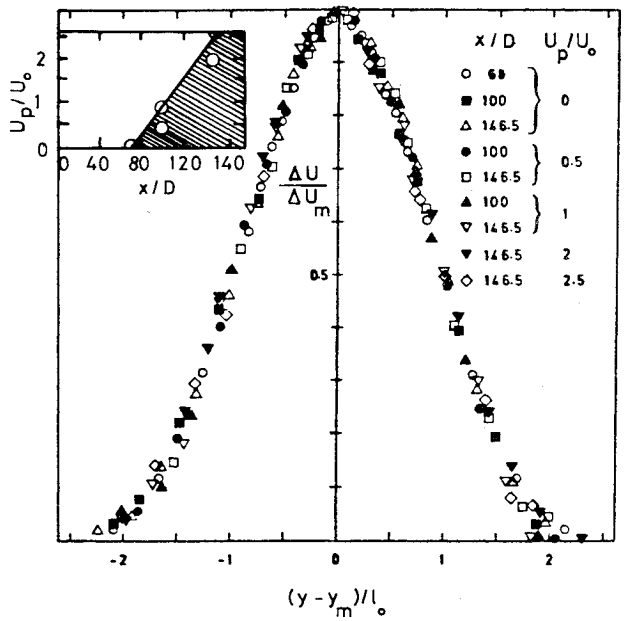

Fig. 5 Normalized mean streamwise velocity profiles.

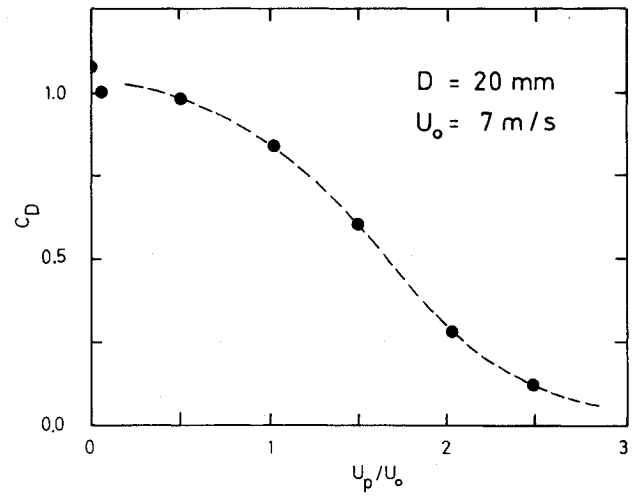

Fig. 6 Drag coefficient as a function of U_p/U_0.

is opposite that of U_0. As x/D increases, the zones of accelerated and decelerated wake flow become smaller and eventually disappear due to lateral momentum transfer and entrainment.

Figure 3 shows in detail the variation of the maximum value of the mean velocity defect ΔU_m with x/D for several values of U_p/U_0. As pointed out, ΔU_m decreases as U_p/U_0 increases for all x/D. The variation of $(U_0/\Delta U_m)^2$ with x/D is linear for any peripheral velocity. The slope of this linear relationship increases rapidly with cylinder rotation, especially for peripheral velocities larger than the freestream velocity, because of the increasingly weaker wake formed when no Kármán vortices are shed from the cylinder for U_p/U_0 in excess of one.[9] The corresponding variation of the characteristic half-wake width ℓ_0 with x/D is depicted in Fig. 4. For U_p/U_0 up to one, ℓ_0 remains approximately constant at any given downstream station; for U_p/U_0 above one, ℓ_0 decreases sharply with rotation; and for $U_p/U_0 \geqq 1.5$, the decrease of ℓ_0 with rotation is quasilinear. This behavior is in agreement with and supports the Kármán vortex shedding results reported in Ref. 9, which indicate that for $U_p/U_0 \leqq 1$ vortex activity remains practically unaffected by rotation and that for $U_p/U_0 > 1.5$ no Kármán vortices are formed and shed. Note that the initial wake width is dominated by the presence and size of the Kármán vortices. Nevertheless, the length scale ℓ_0 shows the expected variation with longitudinal position x/D as $(\ell_0/D)^2$ varies linearly with x/D for any U_p/U_0.

The evolution of the wake mean velocity field toward symmetry is illustrated in Fig. 5, where the normalized mean streamwise velocity profiles are plotted for various values of U_p/U_0 and downstream stations. The profiles have been normalized with respect to the characteristic wake width ℓ_0 and mean velocity defect ΔU_m. The lateral displacement of the wake due to the cylinder rotation has been accounted for by referring lateral positions to y_m. It is clear that these profiles are self-similar and well described by the equation proposed by Townsend,[10]

$$\frac{\Delta U}{\Delta U_m} = \exp\left\{-0.6619\left(\frac{y}{\ell_0}\right)^2\left[1 + 0.0565\left(\frac{y}{\ell_0}\right)^4\right]\right\} \quad (1)$$

Figure 5 also shows that the downstream position at and beyond which the profiles become self-similar depends on U_p/U_0 because the degree of asymmetry is different, increasing as U_p/U_0 increases. For instance, for $U_p/U_0 = 0$ self-similarity is attained at $x/D \cong 60$, whereas for $U_p/U_0 = 2.5$ it is reached at $x/D \cong 150$.

The evolution of the drag coefficient C_D with U_p/U_0 is shown in Fig. 6. This coefficient decreases as U_p/U_0 increases, in accordance with the variation of the wake mean scales ΔU_m and ℓ_0 presented in Figs. 3 and 4. For $1 < U_p/U_0 < 2$, the drag coefficient decreases sharply with increasing peripheral velocity because of the aforementioned change that occurs in

the process of wake formation when $U_p/U_0 > 1$. Not only does the energy of the vortices drop when $U_p/U_0 > 1$, but also the shedding process becomes rapidly randomized with increasing peripheral velocity and, therefore, all dynamic scales of the wake must drop.[9]

The Fluctuating Velocity Field

Figure 7 presents the lateral distributions of the rms streamwise velocity component $(\overline{u^2})^{\frac{1}{2}}$ pertaining to values of U_p/U_0 between 0 and 2.5 and measured at three different stations, $x/D = 10$, 30, and 68. Near the stationary cylinder, $x/D = 10$ and $U_p/U_0 = 0$, the wake is dominated by the passage of Kármán vortices and, as expected, the longitudinal intensities are high. Comparable high levels of velocity fluctuations are obtained at $x/D = 10$ for $U_p/U_0 = 0.5$ and 1.0, especially in the lower region of the flow (which is identified with the bottom of the cylinder where the direction of U_p is opposite to that of U_0). Also, the lateral extent of the fluctuating velocity field remains practically equal in size to that of the stationary cylinder case, indicating that Kármán vortex activity is not much affected by rotation for $U_p/U_0 \leqq 1.0$. When the peripheral velocity exceeds that of the freestream, the longitudinal intensities drop substantially as does the width of the fluctuating field. These results are entirely consistent with the spectral and correlation data for this flow,[9] which establish that the dominant feature of the initial wake development, i.e., the passage of Kármán vortices, is inhibited or disappears when $U_p/U_0 > 1.0$. Similar trends are observed for the two other downstream positions, $x/D = 30$ and 68, included in Fig. 7 except that, as expected, the level of $\overline{u^2}$ decreases with x/D due to the diffusional processes acting within the wake. Note that as the rotational speed increases, the wake is progressively displaced in a lateral direction, which is consistent with the sense of the cylinder rotation. For relatively high rotational speeds ($U_p/U_0 > \sim 2.0$), the form of the asymmetrical $(\overline{u^2})^{\frac{1}{2}}$ profiles changes slightly, since maximum $(\overline{u^2})^{\frac{1}{2}}$ values occur in the upper region of the flow (which is identified with the top

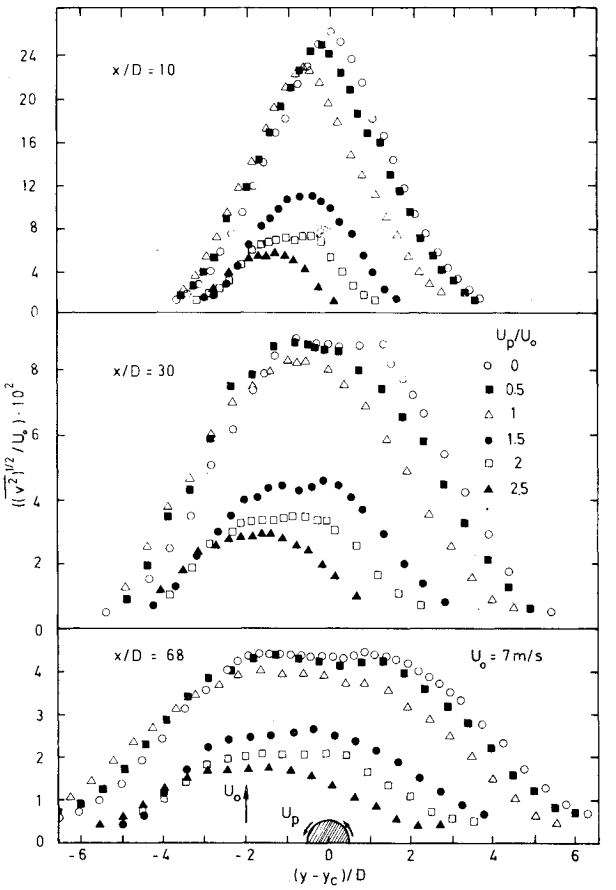

Fig. 8 Lateral turbulence intensity profiles.

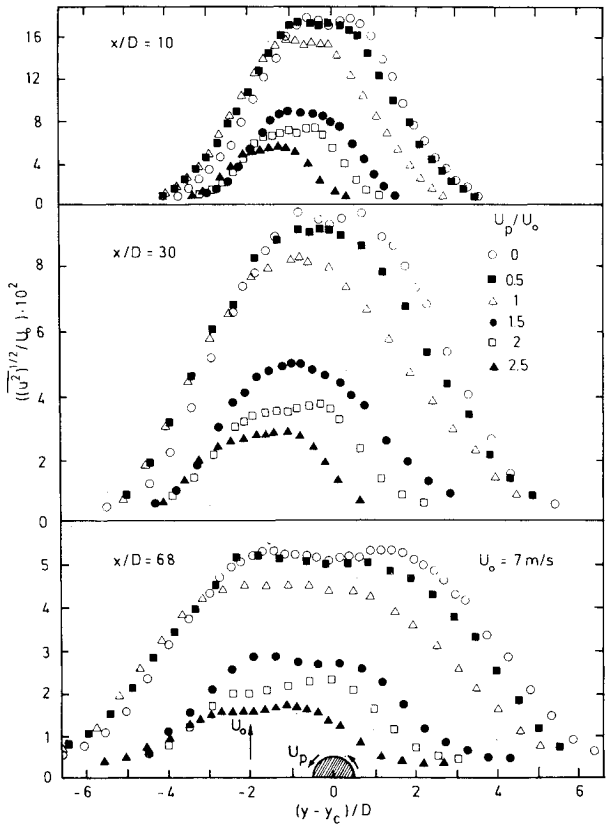

Fig. 7 Streamwise turbulence intensity profiles.

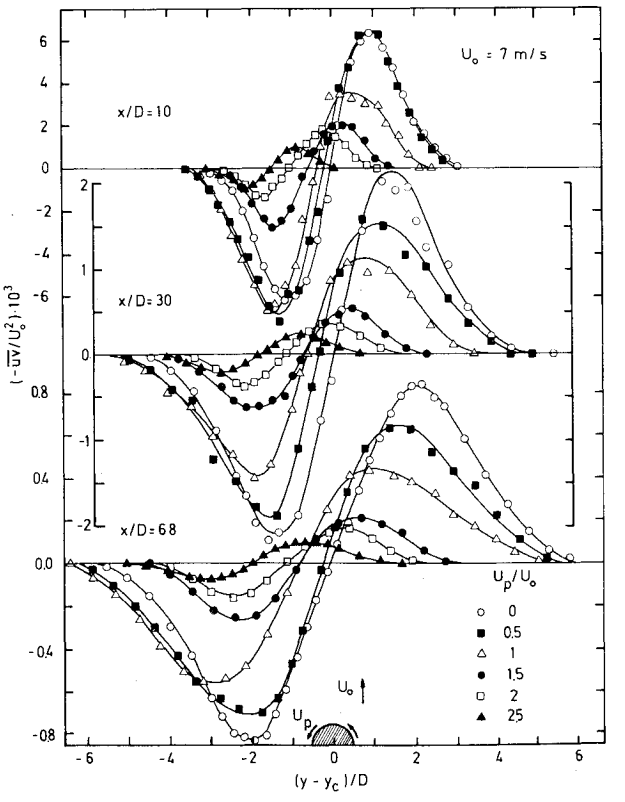

Fig. 9 Reynolds shear stress profiles.

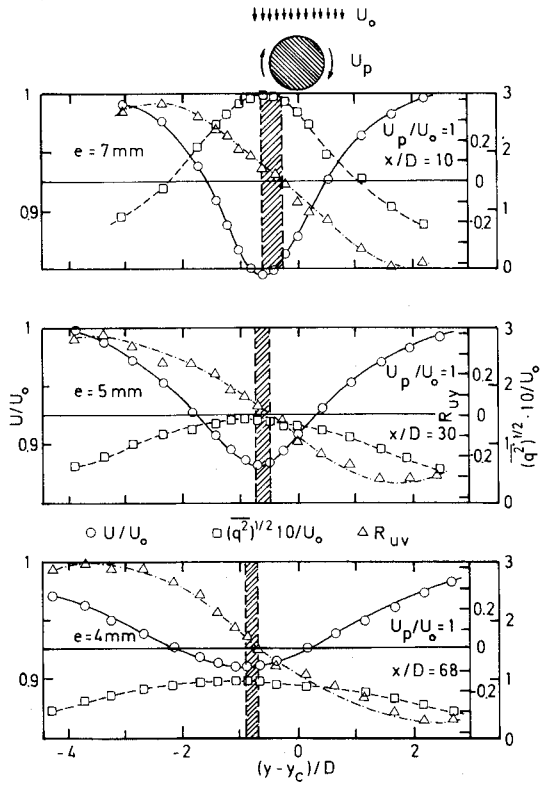

Fig. 10 Distributions of mean velocities, *uv* cross-correlation coefficients, and q'.

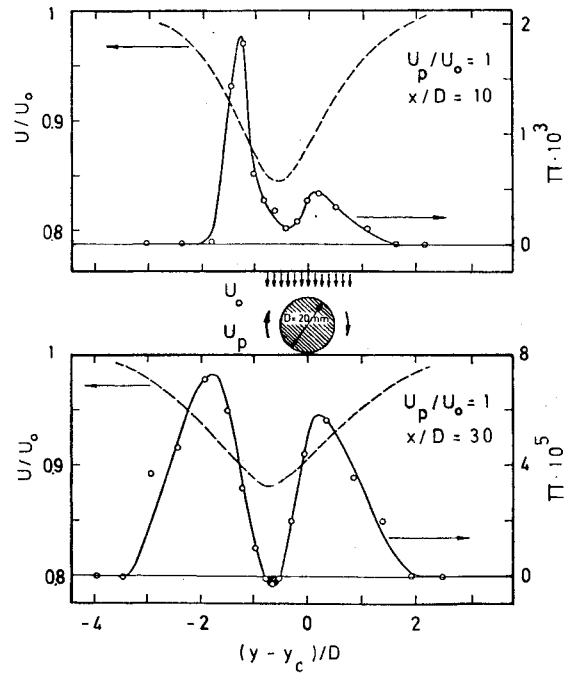

Fig. 11 Lateral distributions of the turbulent kinetic energy production term.

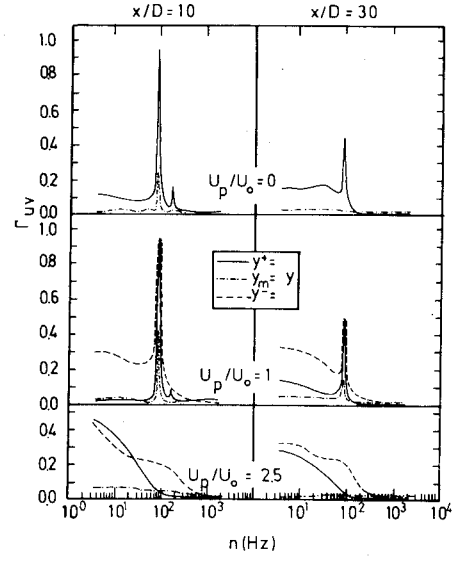

Fig. 12 One-point coherence function of streamwise and lateral velocities.

of the cylinder where the direction of U_p is the same as that of U_0), instead of occurring in the lower region where high shearing action exists, as may be clearly seen in Fig. 7 for $x/D = 40$ and 68. This change is probably due to the initially high compression of the streamlines within the lower region of the flow for high rotational speeds and to the lateral expansion of these streamlines that takes place downstream as the relatively weak wake, free from Kármán vortices, recovers from the initial lateral deflection and evolves toward equilibrium and symmetry.

The lateral distributions of the rms lateral velocity component $(\overline{v^2})^{\frac{1}{2}}$ measured at $x/D = 10$, 30, and 68 are plotted in Fig. 8 for all rotational speeds studied. These profiles display characteristics and trends similar to those just presented and discussed with respect to $(\overline{u^2})^{\frac{1}{2}}$. But for $U_p/U_0 < 1.0$, the lateral intensities are higher than the corresponding longitudinal ones near the cylinder ($x/D = 10$). This is due to the higher sensitivity of $(\overline{v^2})^{\frac{1}{2}}$ to the well-defined Kármán vortices that are convected under these flow conditions. (Note that the mean lateral velocity is small compared to the longitudinal one.) The corresponding shear stress profiles given in Fig. 9 agree with the fluctuating velocity results shown in Figs. 7 and 8. The rms shear stress profiles also indicate that the shearing action in the wake and its lateral extent decrease significantly for $U_p/U_0 > 1.0$. The level of the stresses are higher in the lower region of flow, as expected, and the points of zero stress are laterally displaced in accordance with the sense of the cylinder rotation. The sharp decrease in $\overline{uv}$ with increasing x/D results from the diffusional processes acting in the wake.

A comparison of the mean longitudinal velocity and shear stress profiles, measured in the region of the wake where asymmetry is important, shows that there exist several zones of displacement between the zero of the lateral gradient of the mean longitudinal velocity and the zero of the turbulent shear stress. The displacement zones detected for $U_p/U_0 = 1.0$ at $x/D = 10$, 30, and 68 are illustrated in Fig. 10, where compounded plots of mean velocities, cross-correlation coefficients, and turbulent kinetic energies are presented. The large size of the displacement zone that exists at $x/D = 10$ and its subsequent evolution may be explained by the large degree of asymmetry and local nonequilibrium that rotation imposes on the initial development of the flow through the lateral displacement of the wake and the formation and existence of Kármán vortices of different sizes and energies within the upper and lower regions of the wake. As a consequence, models based on local equilibrium hypotheses, such as that of Boussinesq, become physically unrealistic and inapplicable. References 11-13 have shown that the role of different sizes of coherent structures is predominant with respect to the dynamics of the flow and that it is necessary to postulate at least a bimodal transport mechanism.

The results plotted in Fig. 10 indicate that the direction of the displacement of the zero of R_{uv}, $y_{\overline{uv}=0}$, with respect to the zero of $\partial U/\partial y$, $y_{\partial U/\partial y=0}$, is consistent with the lateral gradient of turbulent energy $\overline{q^2}$, as suggested by[14]

$$e = y_{\overline{uv}=0} - y_{\partial U/\partial y=0} \propto \frac{\partial}{\partial y}\left(\overline{q^2}\right)^{\frac{1}{2}} \qquad (2)$$

Note in Fig. 10 that as the wake is convected downstream, far from the initial asymmetric conditions, and evolves toward the equilibrium between the mean and the fluctuating fields, the size of the displacement zones diminishes, as does the lateral gradient of $\overline{q^2}$, which is also in agreement with Eq. (2).

The lateral distributions of the turbulent kinetic energy production term π, pertaining to $U_p/U_0 = 1.0$ and to values of x/D equal to 10 and 30, are shown in Fig. 11. Both profiles are asymmetrical, especially the one corresponding to $x/D = 10$. The π distribution at $x/D = 30$ presents a negative total production term, defined by

$$\pi = -\left(\overline{uv}\frac{\partial U}{\partial y} + \left(\overline{u^2} - \overline{v^2}\right)\frac{\partial U}{\partial x}\right) \tag{3}$$

within the zone bounded by $y_{\overline{uv}=0}$ and $y_{\partial U/\partial y=0}$. The reason why π becomes negative in the displacement zone at positions x/D greater than 25 is that the fluctuating intensity $\overline{u^2}$ becomes greater than $\overline{v^2}$ for $U_p/U_0 = 1.0$ away from the cylinder, where Kármán vortex activity diminishes and the signs of two terms of Eq. (3) coincide.

Figure 12 depicts the coherence functions of the two velocity components u and v measured at $x/D = 10$ and 30 for different values of U_p/U_0 and selected lateral positions. Here y^+ and y^- refer to the lateral locations at which the magnitude of $\overline{uv}$ is maximum in the upper and lower parts of the wake as sketched in Fig. 1. For U_p/U_0 up to 1, the coherence function displays at y^+ and y^- a sharp peak at the Kármán vortex Strouhal frequency n_S. However, for peripheral velocities larger than $1.5U_0$, no sharp peak exists in the coherence spectrum, indicating the absence of Kármán vortex street activity in the wake. It may be remarked that the magnitude of the coherence peak for U_p/U_0 less than unity decreases substantially between $x/D = 10$ and 30. These results are similar to those found by Budny et al.[15] in the wake behind a stationary cylinder and are in accordance with the fact that Kármán vortex street activity that exists for $U_p/U_0 \leqq 1.0$ decays with increasing x/D.

Conclusion

An experimental investigation has been carried out to characterize the development of a two-dimensional turbulent wake generated by a rotating cylinder. Velocity measurements show that the rotation of the cylinder results in a lateral displacement of the near-wake flow. When the initial curvature of the wake centerline disappears, the lateral displacement diminishes slightly with longitudinal position and the flow evolves toward symmetrical conditions around a plane parallel to, but progressively separated from that of a symmetrical wake, as the rotational speed increases. For peripheral velocities less than the freestream velocity, the characteristic velocity and length scales for the mean flow are effectively equal to those of the stationary cylinder wake, because the shedding of Kármán vortices remains unaffected by rotation. A similar behavior is observed for the fluctuating velocity field at these low rotational speeds. As the peripheral velocity increases beyond that of the oncoming freestream, however, the formation of Kármán vortices is inhibited and the values of the mean velocity defect, wake width, intensities of the fluctuating velocity components, and cross correlations decrease appreciably. Several zones of displacement between the zero of the lateral gradient of the mean longitudinal velocity component and the zero of the Reynolds shear stress have been detected, the largest occurring at $U_p/U_0 = 1.0$. For $x/D \geqq 25$ ($\overline{u^2} \geqq \overline{v^2}$), the net production term of turbulence kinetic energy within some of these localized zones becomes negative.

Acknowledgments

This research was financially supported by CIRIT (Generalitat de Catalunya) and the Canadian Natural Sciences and Engineering Research Council under Grant A2746.

References

[1] Eskinazi, S. and Yeh, H., "An Investigation on Fully Developed Turbulent Flows in a Curved Channel," *Journal of the Aeronautical Sciences*, Vol. 23, 1956, p. 23.

[2] Béguier, C., "Ecoulements Dissymetriques en Regime Turbulent," *Comptes Rendus de l'Academie Sciences, Paris*, Vol. A260, 1965, p. 5460.

[3] Tailland, A. and Mathieu, J., "Jet Pariétal," *Journal de Mécanique*, Vol. 6, No. 1, 1967, pp. 103-131.

[4] Wilson, D.J., "Turbulent Transport of Mean Kinetic Energy in Countergradient Shear Stress Regimes," *Physics of Fluids*, Vol. 17, 1974, p. 674.

[5] Palmer, M.D. and Keffer, J.F., "An Experimental Investigation of an Asymmetrical Turbulent Wake," *Journal of Fluid Mechanics*, Vol. 53, 1972, p. 593.

[6] Giralt, F., Fraunié, P., Béguier, C., and Keffer, J.F., "Energy Reversal in the Wake of Two Cylinders," Paper presented at XV International Congress on Theoretical and Applied Mechanics, Toronto, 1980.

[7] Béguier, C., Giralt, F., Fraunié, P., and Keffer, J.F., "Flux a Contre-Gradient en Aval de Deux Cylindres de Diametres Différents," *Comptes Rendus de l'Academie Sciences, Paris*, Vol. B289, 1979, p. 301.

[8] Diaz, F., "Estela Asimètrica Generada per un Cilindre en Rotació," Doctoral Thesis, Universitat de Barcelona, Spain, 1982.

[9] Diaz, F., Gavaldà, J., Kawall, J.G., Keffer, J.F., and Giralt, F., "Vortex Shedding from a Spinning Cylinder," *Physics of Fluids*, Vol. 26, 1983, p. 3454.

[10] Townsend, A.A., *The Structure of Turbulent Shear Flows*, Cambridge University Press, Cambridge, England, 1976.

[11] Béguier, C., Fulachier, L., and Keffer, J.F., "The Turbulent Mixing Layer with an Asymmetrical Distribution of Temperature," *Journal of Fluid Mechanics*, Vol. 88, 1978, p. 561.

[12] Keffer, J.F., Kawall, J.G., Giralt, F., and Béguier, C., "Analysis of Turbulent Structures in Complex Shear Flows," Paper presented at 2nd Symposium on Turbulent Shear Flows, Imperial College, London, 1979.

[13] Keffer, J.F., Kawall, J.G., Giralt, F., and Béguier, C., "Characteristics of Coherent Structures in Complex Turbulent Shear Flows," Paper presented at International Congress on Heat Transfer and Turbulence Structure (ICHMT/IUTAM), Dubrovnik, Yugoslavia, 1980.

[14] Béguier, C., Giralt, F., Fulachier, L., and Keffer, J.F., "Negative Production in Turbulent Shear Flows," *Lecture Notes in Physics*, Vol. 76, 1977, p. 22.

[15] Budny, R.S., Kawall, J.G., and Keffer, J.F., "Vortex Street Evolution in the Wake of a Circular Cylinder," Paper presented at 2nd International Symposium on Turbulent Shear Flows, Imperial College, London, 1979.